

Deformed shell model study of event rates for WIMP- ^{73}Ge scattering

R. Sahu^{1*} and V.K.B. Kota^{2†}

¹ *National Institute of Science and Technology, Palur Hills, Berhampur-761008, Odisha, India and*

² *Physical Research Laboratory, Ahmedabad 380 009, India*

(Dated: October 17, 2018)

The event detection rates for the WIMP (a dark matter candidate) are calculated with ^{73}Ge as the detector. The calculations are performed within the deformed shell model (DSM) based on Hartree-Fock states. First the energy levels and magnetic moment for the ground state and two low lying positive parity states for this nucleus are calculated and compared with experiment. The agreement is quite satisfactory. Then the nuclear wave functions are used to investigate the elastic and inelastic scattering of WIMP from ^{73}Ge . The nuclear structure factors which are independent of supersymmetric model are also calculated as a function of WIMP mass. The event rates are calculated for a given set of SUSY parameters. The calculation shows that ^{73}Ge is a good detector for detecting dark matter.

PACS numbers: 21.60.Jz, 95.35.+d, 27.50.+e

I. INTRODUCTION

There are overwhelming evidences for the existence of dark matter in the universe [1, 2]. However, it has not yet been observed in earth-bound experiments nor created at particle colliders. The existence of dark matter can be inferred from the rotation curves for spiral galaxies, gravitational lensing in clusters of galaxies, anisotropy in the cosmic microwave background radiation etc. The standard model of cosmology indicates that universe hardly contains $\sim 5\%$ luminous matter, the remainder is 23% non-luminous dark matter and 72% dark energy. The data from the Cosmic Background Explorer (COBE) [3] and Supernova Cosmology project [4] suggest that most of the dark matter is cold. Hot dark matter which is moving at relativistic speed can not cluster on galaxy scale. Up to now, the nature of this matter remains a mystery. The baryonic cold dark matter component can be massive compact halo objects (MACHOs) like neutron stars, white dwarfs, jupiters etc. and results of experimental searches suggest that MACHO fraction should not exceed 20% [1]. Super symmetric theories of physics beyond the standard model provide the most promising nonbaryonic candidates for dark matter. In the simple picture, the dark matter in the galactic halo is assumed to be Weakly Interacting Massive Particles (WIMP). These particles undergo weak interaction and experience the effects of gravity but do not participate in electromagnetic or strong interactions. The most appealing WIMP candidate for nonbaryonic cold dark matter is the lightest super symmetric particle (LSP) which is expected to be a neutral Majorana fermion travelling with non-relativistic velocities. In recent years, there have been considerable theoretical and experimental efforts to detect the WIMP [5].

Since the WIMP (represented by χ) interacts very weakly with matter, its detection is quite difficult. One possibility to detect WIMP is through the recoil of the nucleus in WIMP-nucleus elastic scattering. Popular detector nuclei are ^2He , ^{19}F , ^{23}Na , ^{27}Al , ^{29}Si , ^{40}Ca , ^{73}Ge , ^{75}As , ^{127}I , ^{134}Xe and ^{208}Pb [6]. In WIMP-nucleus scattering, one should consider, in addition to the scalar interaction, the spin-spin interaction in which the WIMP couples to the spin of the nucleus. Exotic WIMPs can lead to large nucleon spin induced cross sections which in turn can lead to non-negligible probability for inelastic WIMP-nucleus scattering [5] provided the energy of the excited state is sufficiently low as in the $7/2^+$ state of ^{73}Ge . Many such nuclei with excited state very close to the ground state, have recently been studied, for example ^{83}Kr [5], ^{83}Kr and ^{125}Te [7], ^{127}I , ^{129}Xe , ^{131}Xe and ^{133}Cs [8] etc.

There are many experimental efforts to directly detect dark matter by trying to measure the energy deposited when a WIMP from the Galactic halo scatters from a nucleus in the detector. Because of the low count rates, the choice of the detector becomes very important. Searches for spin-dependent interactions require the use of targets with nonzero spin. There are many advantages in choosing lighter target like ^{73}Ge as a detector. It is better for detecting light mass dark matter. It is also stable, its natural abundance is 7.75%. Hence the cost of making the target can be considerably reduced by choosing this nucleus. Again the low lying excited state $7/2^+$ at 0.0687 MeV and half-life of 174 ns can open up new possibilities for spin dependent inelastic WIMP-nucleus scattering which can be sizable. The Cryogenic Dark Matter Search (CDMS) experimental facility [9] is designed to directly detect the dark matter with ^{73}Ge as the target nucleus. It has set the most sensitive limits on the interaction of WIMP with terrestrial materials. The development of upgrades is underway and will be located at SNOLAB. Another dark matter experiment is EDELWEISS facility in France [10] which uses high purity germanium cryogenic bolometers at milikelvin tem-

*rankasahu@gmail.com

†vkbkota@prl.res.in

peratures. There are also other experimental attempts using detectors like ^{19}F , ^{127}I , $^{129,131}\text{Xe}$, ^{133}Cs etc. see for details [11].

The count rate in WIMP-nucleus scattering experiences an annual modulation as a result of the earth's orbital motion around the sun. The Milky Way is assumed to be surrounded by a halo of non-rotating dark matter. As the solar system moves through the Milky Way, it experiences a wind of dark matter. The earth moves against the wind for half of the year and experiences the minimum wind velocity on December 2. The wind velocity increase as the earth moves in the opposite direction attaining maximum value on June 2. Annual modulation is a powerful signature for the existence of dark matter since such modulation is not exhibited by the background radiation. The DAMA experiments [12] have claimed the observation of the annual modulation of a dark matter signal. However this claim has been contested by many other experiments. In view of the above, it will be interesting to study the annual modulation of the event rates theoretically.

The nuclear structure effects are important and should be incorporated in many of the astro-particle physics problems. The nuclear model should be first tested regarding its success in describing the properties of nuclei before applying it to problems like dark matter detection. The deformed shell model (DSM), based on Hartree-Fock (HF) deformed intrinsic states with angular momentum projection and band mixing, is established to be a good model to describe the properties of nuclei in the mass range $A=60-100$. See [13] for details regarding DSM and its applications. The model is found to be quite successful in describing spectroscopic properties including spectroscopy of $N=Z$ odd-odd nuclei with isospin projection see for example [14], double beta decay half-lives [15, 16], $\mu - e$ conversion in the field of the nucleus [17] and so on. It will be quite interesting to employ DSM to calculate the detection rates for the lightest super symmetric particle (a dark matter candidate) with ^{73}Ge as the detector. In addition to the elastic scattering, the inelastic scattering of WIMP from ^{73}Ge , which has not been studied up to now, will also be considered in this article.

Regarding other theoretical works, it may be mentioned that truncated shell model calculations have been carried out for the studies of event rates with the detectors ^{83}Kr [5], ^{83}Kr and ^{125}Te [7], ^{127}I , ^{129}Xe , ^{131}Xe and ^{133}Cs [8] etc. In these publications, both the event rates for elastic and inelastic WIMP-nucleus scattering have been considered. The annual modulation of signals are also considered. The event rates and annual modulation signals for ^{23}Na , ^{71}Ga , ^{73}Ge and ^{127}I cold dark matter detectors have been studied using the truncated shell model [21]. However, in this study the authors restricted to only elastic scattering. Using the quasi-particle phonon model, Holmlund et al.[22] have studied the elastic WIMP detection rates for ^{71}Ga , ^{73}Ge and ^{127}I dark matter detectors. There are also calculations of spin-dependent and spin-independent WIMP

currents in nuclei based on chiral effective field theory using large-scale shell model [23–25]. The structure factors for spin-independent WIMP scattering off xenon has been recently calculated within the shell model[26]. In these shell model calculations truncation of the valance space has been done to bring the matrix dimensions to a manageable size.

Section II gives some details regarding DSM and also about the formulation of WIMP-nucleus scattering event rates. The spectroscopic results and also the results for elastic and inelastic scattering of WIMP from ^{73}Ge are discussed in Section III. Finally, concluding remarks are drawn in Sect. IV.

II. EVENT RATES FOR WIMP-NUCLEUS SCATTERING

Direct detection of WIMP is most interesting since the earth is washed with millions of WIMPs every second coming from the galactic halo. The nuclear recoil in the WIMP-nucleus scattering can be measured with suitable detectors. The relevant theory of WIMP-nucleus scattering are discussed below. In the expressions for the event rates, the super-symmetric part is separated from the nuclear part so that the role played by the nuclear part becomes apparent. The nuclear structure calculations are performed within our deformed shell model based on Hartree-Fock states.

A. Elastic scattering

The differential event rate per unit detector mass can be written as [1]

$$dR = N_t \phi \frac{d\sigma}{d|q|^2} f d^3v d|q|^2 \quad (1)$$

In the above equation, N_t stands for the number of target nuclei per unit mass which is equal to $1/(Am_p)$, A being the mass number of the nucleus in the detector and m_p is the proton mass. ϕ is the dark matter flux which is equal to $\rho_0 v/m_\chi$. ρ_0 is the local WIMP density and m_χ is the WIMP mass. f takes into account the distribution of the WIMP velocity relative to the detector (or earth) and also the motion of the sun and earth. The distribution is assumed to be Maxwell-Boltzmann type. If we neglect the rotation of earth in its own axis, then $v = |\mathbf{v}|$ is the relative velocity of WIMP with respect to the detector. q represents the momentum transfer to the nuclear target. Introducing the dimensionless variable $u = q^2 b^2/2$ with b as the oscillator length parameter, the WIMP-nucleus differential cross section in the laboratory frame is given by [7, 8, 21, 22]

$$\frac{d\sigma(u, v)}{du} = \frac{1}{2} \sigma_0 \left(\frac{1}{m_p b} \right)^2 \frac{c^2}{v^2} \frac{d\sigma_A(u)}{du}; \quad (2)$$

with

$$\frac{d\sigma_A(u)}{du} = [f_A^0 \Omega_0(0)]^2 F_{00}(u) + 2f_A^0 f_A^1 \Omega_0(0) \Omega_1(0) F_{01}(u) + [f_A^1 \Omega_1(0)]^2 F_{11}(u) + M^2. \quad (3)$$

In Eq. (3), the first three terms correspond to spin contribution coming from the axial current and the fourth term stands for the coherent part coming mainly from the scalar interaction. The coherent part can be described in terms of the nuclear form factors given as

$$M^2 = (f_S^0 [ZF_Z(u) + NF_N(u)] + f_S^1 [ZF_Z(u) - NF_N(u)])^2 \quad (4)$$

If the proton and neutron form factors $F_Z(u)$ and $F_N(u)$ are nearly equal, then taking $F_Z(u) \approx F_N(u) = F(u)$, we have

$$M^2 = A^2 \left(f_S^0 - f_S^1 \frac{A-2Z}{A} \right)^2 |F(u)|^2. \quad (5)$$

Here, f_A^0 and f_A^1 represent isoscalar and isovector parts of the axial vector current and similarly f_S^0 and f_S^1 represent isoscalar and isovector parts of the scalar current. These nucleonic current parameters depend on the specific SUSY model employed. The spin structure functions $F_{\rho\rho'}(u)$ with $\rho, \rho' = 0,1$ are defined as

$$F_{\rho\rho'}(u) = \sum_{\lambda,\kappa} \frac{\Omega_\rho^{(\lambda,\kappa)}(u) \Omega_{\rho'}^{(\lambda,\kappa)}(u)}{\Omega_\rho(0) \Omega_{\rho'}(0)}; \quad (6)$$

$$\Omega_\rho^{(\lambda,\kappa)}(u) = \sqrt{\frac{4\pi}{2J_i+1}}$$

$$\times \langle J_f || \sum_{j=1}^A [Y_\lambda(\Omega_j) \otimes \sigma(j)]_{\kappa} j_\lambda(\sqrt{u} r_j) \omega_\rho(j) || J_i \rangle$$

with $\omega_0(j) = 1$ and $\omega_1(j) = \tau(j)$; note that $\tau = +1$ for protons and -1 for neutrons. Here Ω_j is the solid angle for the position vector of the j -th nucleon and j_λ is the spherical Bessel function. The static spin matrix elements are defined as $\Omega_\rho(0) = \Omega_\rho^{(0,1)}(0)$. The distribution function f is given by [7]

$$f(\mathbf{v}, \mathbf{v}_E) = \frac{1}{(\sqrt{\pi} v_0)^3} e^{-(\mathbf{v}+\mathbf{v}_E)^2/v_0^2} \quad (7)$$

In the above equation (7), \mathbf{v} is the velocity of WIMP with respect to the earth containing the detector and \mathbf{v}_E is the velocity of the earth with respect to the galactic center given as

$$\mathbf{v}_E = \mathbf{v}_0 + \mathbf{v}_1. \quad (8)$$

In the above \mathbf{v}_0 stands for the velocity of the sun with respect to the galactic centre and \mathbf{v}_1 is the velocity of earth with respect to the sun. Assuming that the polar axis is

aligned along the direction of \mathbf{v}_1 and converting the integration variables into dimensionless form, the event rate is obtained by integrating Eq. (1) with respect to u , velocity v and angle θ and can be written as

$$\langle R \rangle = \int_{-1}^1 d\xi \int_{\psi_{min}}^{\psi_{max}} d\psi \int_{u_{min}}^{u_{max}} G(\psi, \xi) \frac{d\sigma_A(u)}{du} du \quad (9)$$

In the above, $G(\psi, \xi)$ is given by

$$G(\psi, \xi) = \frac{\rho_0}{m_\chi} \frac{\sigma_0}{Am_p} \left(\frac{1}{m_p b} \right)^2 \frac{c^2}{\sqrt{\pi} v_0} \psi e^{-\lambda^2} e^{-\psi^2} e^{-2\lambda\psi\xi} \quad (10)$$

Here, $\psi = v/v_0$, $\lambda = v_E/v_0$, $\xi = \cos(\theta)$. The values of the parameters used in the calculation are the following: the WIMP density $\rho_0 = 0.3 \text{ GeV/cm}^3$, $\sigma_0 = 0.77 \times 10^{-38} \text{ cm}^2$, mass of proton $m_p = 1.67 \times 10^{-27} \text{ kg}$. m_χ is the WIMP mass. The velocity of the sun with respect to the galactic centre is taken to be $v_0 = 220 \text{ Km/s}$ and the velocity of the earth relative to the sun is taken as $v_1 = 30 \text{ Km/s}$. The velocity of the earth with respect to the galactic centre v_E is given by

$$v_E = \sqrt{v_0^2 + v_1^2 + 2v_0 v_1 \sin(\gamma) \cos(\alpha)} \quad (11)$$

α is the modulation angle which stands for the phase of the earth on its orbit around the sun and γ is the angle between the normal to the elliptic and the galactic equator which is taken to be $\simeq 29.8^\circ$. The value of the oscillator length parameter is taken to be 1.91 fm. In our earlier work in the calculation of transition matrix elements for $\mu - e$ conversion in ^{72}Ge [17], we had taken the value of this length parameter as 1.90 fm. Assuming the $A^{1/6}$ dependence, the value for ^{73}Ge is taken to be slightly different 1.91 fm. Writing $\frac{d\sigma_A}{du}$ from Eq. (3) in the form

$$\frac{d\sigma_A(u)}{du} = (f_A^0)^2 X(1) + 2f_A^0 f_A^1 X(2) + (f_A^1)^2 X(3) + A^2 (f_S^0 - f_S^1 \frac{A-2Z}{A})^2 X(4) \quad (12)$$

where $X(1) = [\Omega_0(0)]^2 F_{00}(u)$, $X(2) = \Omega_0(0) \Omega_1(0) F_{01}(u)$, $X(3) = [\Omega_1(0)]^2 F_{11}(u)$, $X(4) = [F(u)]^2$, the event rate per unit mass of the detector can be written as

$$\langle R \rangle = (f_1^0)^2 D_1 + 2f_A^0 f_A^1 D_2 + (f_A^1)^2 D_3 + A^2 (f_S^0 - f_S^1 \frac{A-2Z}{A})^2 |F(u)|^2 D_4 \quad (13)$$

D_1, D_2, D_3 are the three dimensional integrations of Eq. (9) involving the first three spin dependent terms of Eq. (3) and D_4 is the integration involving the coherent term.

$$D_i = \int_{-1}^1 d\xi \int_{\psi_{min}}^{\psi_{max}} d\psi \int_{u_{min}}^{u_{max}} G(\psi, \xi) X(i) du \quad (14)$$

The lower and upper limits of integrations given in Eq.(9) and (14) have been worked out by Pirinen et al

[7] and they are

$$\psi_{min} = \frac{c}{v_0} \left(\frac{Am_p Q_{thr}}{2\mu_r^2} \right)^{1/2} \quad (15)$$

$$\psi_{max} = -\lambda\xi + \sqrt{\lambda^2\xi^2 + \frac{v_{esc}^2}{v_0^2} - 1 - \frac{v_1^2}{v_0^2} - \frac{2v_1}{v_0} \sin(\gamma)\cos(\alpha)} \quad (16)$$

Taking the escape velocity v_{esc} from our galaxy to be 625 km/s, the value of $v_{esc}^2/v_0^2 - 1 - v_1^2/v_0^2$ appearing in Eq. (16) is 7.0525. Similarly taking $\gamma = 29.8^\circ$, the value of $(2v_1/v_0)\sin(\gamma)$ is 0.135. The values of u_{min} and u_{max} are

$$u_{min} = Am_p Q_{thr} b^2 \quad (17)$$

$$u_{max} = 2(\psi\mu_r b v_0/c)^2 \quad (18)$$

In the above equations, Q_{thr} is the detector threshold energy and μ_r is the reduced mass of the WIMP-nucleus system.

B. Inelastic scattering

In the inelastic scattering the entrance channel and exit channel are different and hence the coherent part does not contribute to the event rate. Hence the inelastic event rate per unit mass of the detector can be obtained from Eq. (12)

$$\langle R \rangle_{in} = (f_1^0)^2 E_1 + 2f_A^0 f_A^1 E_2 + (f_A^1)^2 E_3 \quad (19)$$

E_1 , E_2 and E_3 are the three dimensional integrations

$$E_i = \int_{-1}^1 d\xi \int_{\psi_{min}}^{\psi_{max}} d\psi \int_{u_{min}}^{u_{max}} G(\psi, \xi) X(i) du \quad (20)$$

The integration limits for E_1 , E_2 and E_3 are [7, 8]

$$u_{min} = \frac{1}{2} b^2 \mu_r^2 \frac{v_0^2}{c^2} \psi^2 \left[1 - \sqrt{1 - \frac{\Gamma}{\psi^2}} \right]^2 \quad (21)$$

$$u_{max} = \frac{1}{2} b^2 \mu_r^2 \frac{v_0^2}{c^2} \psi^2 \left[1 + \sqrt{1 - \frac{\Gamma}{\psi^2}} \right]^2 \quad (22)$$

where

$$\Gamma = \frac{2E^* c^2}{\mu_r c^2 v_0^2} \quad (23)$$

E^* being the energy of the excited state. ψ_{max} is same as in the elastic case and the lower limit $\psi_{min} = \sqrt{\Gamma}$. The values of the parameters like ρ_0 , σ_0 etc. are same as in the elastic case.

C. Deformed shell model

In the calculation of the event rate (both for elastic and inelastic scattering), the nuclear part has been separated from the super-symmetric part in the formulation. The nuclear part enters in the calculation of the nuclear structure factors D_1 , D_2 , D_3 and D_4 in the elastic scattering and the corresponding factors E_1 , E_2 and E_3 in inelastic scattering. The evaluation of these nuclear structure factors in turn depends on spin structure functions and the form factors. We have used our deformed shell model for the evaluation of these quantities. The details of this model have been described in many of our earlier publications, see for example [13]. In this model, for a given nucleus, starting with a model space consisting of the given set of single particle (sp) orbitals and effective two-body Hamiltonian (TBME + spe), the lowest energy intrinsic states are obtained by solving the Hartree-Fock (HF) single particle equation self-consistently. We assume axial symmetry. Excited intrinsic configurations are obtained by making particle-hole excitations over the lowest intrinsic state. These intrinsic states $\chi_K(\eta)$ do not have definite angular momenta. Hence states of good angular momentum projected from an intrinsic state $\chi_K(\eta)$ can be written in the form

$$\psi_{MK}^J(\eta) = \frac{2J+1}{8\pi^2 \sqrt{N_{JK}}} \int d\Omega D_{MK}^{J*}(\Omega) R(\Omega) |\chi_K(\eta)\rangle \quad (24)$$

where N_{JK} is the normalization constant given by

$$N_{JK} = \frac{2J+1}{2} \int_0^\pi d\beta \sin \beta d_{KK}^J(\beta) \langle \chi_K(\eta) | e^{-i\beta J_y} | \chi_K(\eta) \rangle \quad (25)$$

In Eq. (24), Ω represents the Euler angles (α, β, γ) , $R(\Omega)$ which is equal to $\exp(-i\alpha J_z) \exp(-i\beta J_y) \exp(-i\gamma J_z)$ represents the general rotation operator. The good angular momentum states projected from different intrinsic states are not in general orthogonal to each other. Hence they are orthonormalized and then band mixing calculations are performed. DSM is well established to be a successful model for transitional nuclei (with $A=60-90$) [13–15, 18–20].

In the evaluation of the reduced matrix element appearing in Eq. (6) in DSM, we need the sp matrix elements of the operator of the form $t_\nu^{(l,s)J}$ and these are given by,

$$\begin{aligned} \langle n_i l_i j_i || \hat{t}^{(l,s)J} || n_k l_k j_k \rangle = \\ \sqrt{(2j_k+1)(2j_i+1)(2J+1)(s+1)(s+2)} \\ \left\{ \begin{matrix} l_i & 1/2 & j_i \\ l_k & 1/2 & j_k \\ l & s & J \end{matrix} \right\} \langle l_i || \sqrt{4\pi} Y^l || l_k \rangle \langle n_i l_i || j_l(kr) || n_k l_k \rangle. \end{aligned} \quad (26)$$

In the above equation, $\{--\}$ is the nine- j symbol.

III. RESULTS AND DISCUSSIONS

Before carrying out the calculation for event rates in WIMP-nucleus scattering, we first check the goodness of the nuclear wave functions by computing the energy level spectrum and magnetic moments and compare them with experimentally measured quantities. Good agreement with experiment will give us confidence in our results for event rates. In DSM calculations, ^{56}Ni is taken as the inert core with the spherical orbits $1p_{3/2}$, $0f_{5/2}$, $1p_{1/2}$ and $0g_{9/2}$ forming the basis space. Modified Kuo interaction with single particle energies 0.0, 0.78, 1.08 and 4.90 MeV has been used in the calculation. This effective interaction has been used in many of our calculations and has been found to be quite successful in describing most of the important features of nuclei in this region. The HF single particle spectrum obtained by solving the HF equation self-consistently is shown in Fig. 1. The four protons of this nucleus occupy the lowest two $k = 1/2^-$ orbits. On the other hand ten neutrons occupy pf orbits with three remaining neutrons in the $g_{9/2}$ orbit. As described earlier, we have generated three intrinsic states of positive parity and three intrinsic states of negative parity by particle-hole excitation. Good angular momentum states are projected from each of these intrinsic states and then a band mixing calculation is performed. The low-lying levels obtained in the band mixing calculation are compared with experiment as shown in Fig. 2 up to an excitation energy of 1 MeV. The data are taken from ref. [27, 28]. As can be seen, the agreement with experiment is quite satisfactory. The ground state and next two excited states are quite nicely reproduced. However, there are more levels in experiment than in our calculation. This problem can be solved by taking more intrinsic states in our calculation. Since we are concerned with the calculation of event rate for dark matter - nucleus scattering, we are interested only in the ground state for elastic scattering and ground state and an excited state in the inelastic scattering, the intrinsic states taken are expected to be sufficient. The collective bands recently observed by Sun et al [28] are compared with our DSM calculated results in Fig. 3. The agreement is reasonably good. More number of intrinsic states would have improved the results considerably. But our aim here is not to concentrate in detailed spectroscopy and hence taking more intrinsic states to study alignment effects in the collective bands are not necessary.

Since spin contributions play an important role in the calculation of event rates, the calculation of magnetic moment is first carried out. For better physical insight, it is decomposed into orbital and spin parts. The results for the contribution of protons and neutrons to the orbital and spin parts for the first three positive parity levels $9/2^+$, $7/2^+$ and $5/2^+$ are given in Tab. I. The calculated magnetic moments are also compared with experiment. In the calculation, bare values of g-factors has been used and no quenching has been done. The DSM value for the magnetic moment of the ground state $9/2^+$

is $-0.811 \mu_N$ which agrees quite well with the experimental value $-0.879 \mu_N$. The calculated magnetic moment of the lowest $5/2^+$ also agrees quite well with experiment. However no experimental results are available for the first 7^+ level. Holmlund et al. [22] have calculated the magnetic moment and also the decomposed orbital and spin parts for the ground state of this nucleus and compared their results with different theoretical calculations. Our values agree quite well with the shell model results cited in the above publication.

With the success of the DSM model in explaining the low lying energy levels and the magnetic moments of the lowest three positive parity levels, we then proceed to calculate the event rates for the elastic and inelastic scattering with confidence.

A. Results for elastic scattering

Using the DSM wave function, the spin structure functions for the elastic channel are calculated using the formula given in Eq. (6) for the ground state $9/2^+$. The results are plotted in Fig. 4. Similarly the proton and neutron form factors are calculated using Eq. (6) and plotted in Fig. (4). As can be seen, the form factors for protons and neutrons are almost same. Hence the approximation made in deriving the Eq. (5) is correct. We find that F_{00} , F_{01} and F_{11} have almost equal values. The spin structure functions as well as the form factor approach zero for $u > 1$. Hence the main contribution to the event rate comes from the spin structure functions and form factor with $u < 1$. The plot of the spin structure functions is almost similar to results obtained in ref. [22] within their quasi-particle-pairing model. DSM gives the values of static spin matrix elements Ω_0 and Ω_1 to be 0.798 and -0.803. These values agree quite nicely with the results obtained by Kortelainen et al. [21]. Using shell model Ressel et al. [29] have calculated $S_{\rho\rho'}$, that are related to the spin structure functions defined above. Their values compare well with the DSM results.

The coefficients D_1 , D_2 , D_3 and D_4 defined in Eq. (14) depend only on the nuclear wave functions and they are evaluated within our DSM model. Since $\Omega_1(0)$ is negative, the coefficient D_2 is also negative. We plot in Fig. 5 D_1 , $-D_2$, D_3 and D_4 as a function of the WIMP mass for three values of the detector threshold energy $Q_{thr} = 0, 5, 10$ keV. For $Q_{thr} = 0$, all the four graphs peak at WIMP mass ~ 35 GeV. For higher values of Q_{thr} , the peaks shift towards higher WIMP mass. The height of the peaks for D_1 , $-D_2$ and D_3 are smaller than the values reported for ^{83}Kr [7]. However, D_4 is almost similar to ^{83}Kr . The thickness of the graphs represents annual modulation. The modulation signal is large for WIMP mass below ~ 70 GeV. However, modulation effect tapers off at higher values of the WIMP mass. The magnitude of the modulation at WIMP mass ~ 35 GeV is about 3.3% for the spin dependent channels and about 4% for the spin independent case. Thus we predict much

TABLE I: The calculated magnetic moments and their decomposition into orbital and spin parts for ^{73}Ge . The experimental values are given within the parentheses. Bare gyro magnetic ratios have been used in the calculation. The experimental data are from ref. [27].

J	$\langle l_p \rangle$	$\langle S_p \rangle$	$\langle l_n \rangle$	$\langle S_n \rangle$	μ (n.m.)
$9/2^+$	0.581	-0.001	3.558	0.362	-0.811 (-0.879)
$7/2^+$	0.691	-0.009	2.590	0.228	-0.232
$5/2^+$	0.036	0.008	2.189	0.265	-0.929 (-1.080)

smaller modulation compared to ^{83}Kr where it is $\sim 10\%$. At WIMP mass 150 GeV, the modulation effect for the spin independent channel D_4 changes sign. However, no such reversal is found for spin dependent channels. As has been discussed earlier, annual modulation is a powerful signature for the existence of dark matter since such modulations are not exhibited by the back ground. The DAMA experiments [12] had claimed the observation of a positive dark matter signal through the observation of annual modulation over 13 years of operation. However these results are in apparent contradiction with the null results from other experiments like CoGent [30], CDMS [9], XENON [31] experiments. However, the CRESST experiment [32] claims to have observed the modulation. Hopefully in the near future, we will get an unanimous answer regarding the observation of modulation.

Using the values of SUSY parameters $f_A^0 = 3.55e - 2$, $F_A^1 = 5.31e - 2$, $f_S^0 = 8.02e - 4$ and $f_S^1 = -0.15 \times f_S^0$, we have calculated the event rate for the detection WIMP corresponding to the WIMP mass 110 GeV. The results are given in Fig. 6. The thickness of the graph represents annual modulation. The event rate changes drastically depending on the choice of the SUSY parameters [21]. This is because, the expression for event rate can be split into two parts. The spin dependent term is represented by the coefficients $D_{1,2,3}$ and the coherent term represented by D_4 . The different parametrizations weigh these channels differently and hence the different choice of the parameter set gives different results.

B. Results for inelastic scattering

In ^{73}Ge , the first excited positive parity state is $5/2^+$ and scattering to this state from the ground state is not allowed because of mainly the $M1$ type of the interaction. The next excited positive parity state is $7/2^+$ state at an excitation energy of 68.7 keV [28] and scattering to this state is allowed. Unlike the ground state and the first excited positive parity state for which the magnetic moments have been known, the magnetic moment for the $7/2^+$ has not been measured, see Tab. I. The calculated value is $-0.232 \mu_N$ which should be nearer to the actual value since the magnetic moment of the other two lower positive parity states agree so well with experiment.

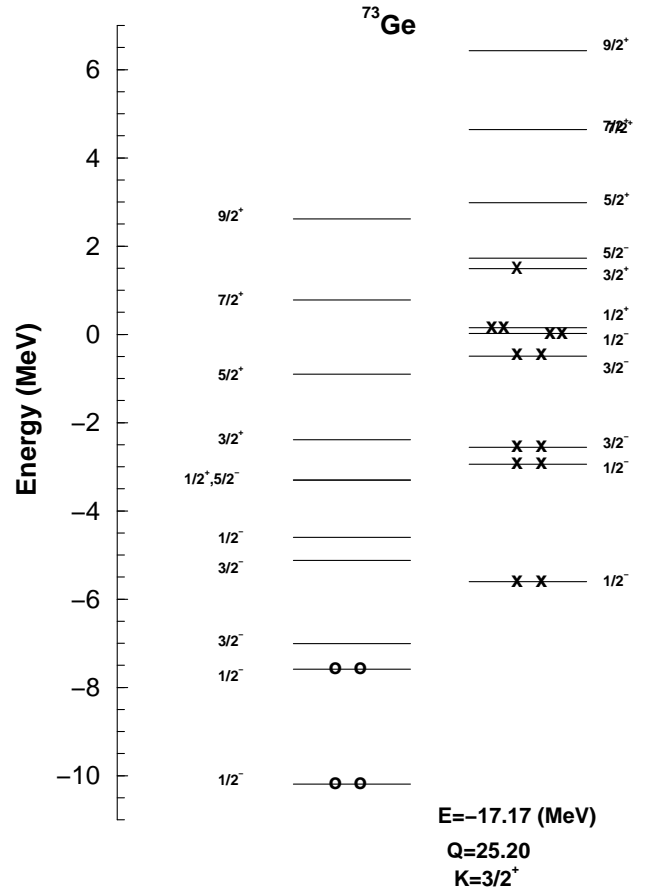


FIG. 1: HF single-particle spectra for ^{73}Ge corresponding to the lowest prolate configuration. In the figure circles represent protons and crosses represent neutrons. The HF energy (E) in MeV, mass quadrupole moment (Q) in units of the square of the oscillator length parameter and the total azimuthal quantum number K are given in the figure.

The static spin matrix elements for the inelastic scattering to the $7/2^+$ state are $\Omega_0 = -0.167$ and $\Omega_1 = 0.142$. These values are about 6–7 times smaller than the corresponding values in the elastic scattering case. However, these values are about 4 times larger than the values quoted for ^{83}Kr [7] obtained within the full shell model with $jj44b$ effective interaction. Our values are almost as large as in ^{125}Te [7] and therefore the inelastic event rate should be competitive. The inelastic spin structure functions are presented in Fig. 7. The structure functions almost overlap with each other except for a small window lying between $0.7 \leq u \leq 4$. In ^{83}Kr , the three structure functions deviate from each other over a longer domain.

The nuclear structure coefficients E_1 , E_2 and E_3 defined in Eq. (20) are calculated and plotted in Fig. 5. The peaks occur at around $m_\chi = 45$ GeV, almost similar to the elastic case. The peak values are almost 13 times larger than the values reported for ^{83}Kr , but about a factor of two smaller than for ^{125}Te [7]. The modulation is about 4% almost similar to the elastic

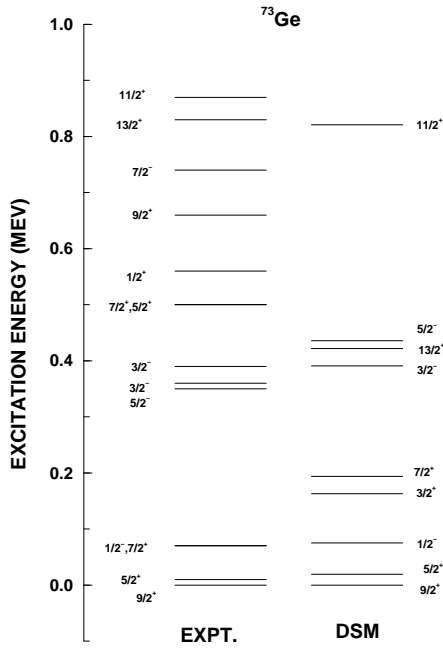


FIG. 2: Comparison of deformed shell model results with experimental data for the low-lying levels. The experimental values are taken from [27]

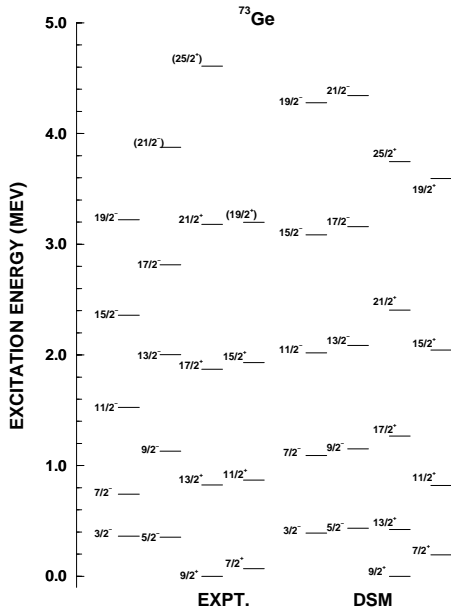


FIG. 3: Comparison of deformed shell model results with experimental data for the collective bands recently observed for this nucleus [28]

case. But for ^{83}Kr and ^{125}Te , Pirinen et al. [7] found the modulation effect to be much larger in the inelastic case than in elastic case. The nuclear structure coefficients do not depend on the detector threshold energy. Hence the event rate can be calculated by reading the values of E_i from the graph and using the SUSY parameters. Because of the large values of E_i , the inelastic scattering of WIMP from ^{73}Ge is a potential candidate for dark matter detection.

IV. CONCLUSIONS

The deformed shell model based on HF states is used to study the event rates for elastic and inelastic scattering of WIMP from ^{73}Ge . First energy spectrum and magnetic moments are calculated to test the goodness of the nuclear wave functions. After ensuring the good agreement with experiment, we studied the event rate. The nuclear structure coefficients and the static spin matrix elements suggest that ^{73}Ge is a good detector for dark matter detection. We have also calculated the annual modulation rates for both elastic and inelastic scattering which is about 3-4% at the peaks. The inelastic scattering of WIMP from ^{73}Ge has been calculated for the first time in this article. The nuclear structure coefficients for this nucleus in the inelastic scattering is much larger than ^{83}Kr and are almost as large as ^{125}Te . Since ^{73}Ge is stable and natural abundance is relatively large, it will be worth while to experimentally study inelastic scattering from this nucleus. The detection of the inelastic event rate will provide information regarding the spin dependent nature of WIMP-nucleus interaction.

Acknowledgments

We are thankful to J.D. Vergados and J. Suhonen for useful correspondence and encouragements. Thanks are also due to T.S. Kosmas for discussions in the initial stages of this work. R. Sahu is thankful to SERB of Department of Science and Technology (Government of India) for financial support.

- [1] G. Jungman, M. Kamionkowski and K. Griest, *Phys. Rep.* **267**, 195 (1996).
- [2] D. Majumdar, Dark matter: An introduction, CRC press, Taylor and Francis group, Florida, (2014).
- [3] G.F. Smoot et al., *Astrophys. J. Lett.* **396**, L1 (1992).

- [4] E. Gawser and J. Silk, *Science* **280**, 1405 (1988).
- [5] J.D. Vergados, F.T. Avignone III, P. Pirinen, P.C. Srivastava, M. Kortelainen and J. Suhonen, *Phys. Rev. D* **92** (2015) 015015/1-13.
- [6] P.C. Divari, T.S. Kosmas, J.D. Vergados and I.D. Sk-

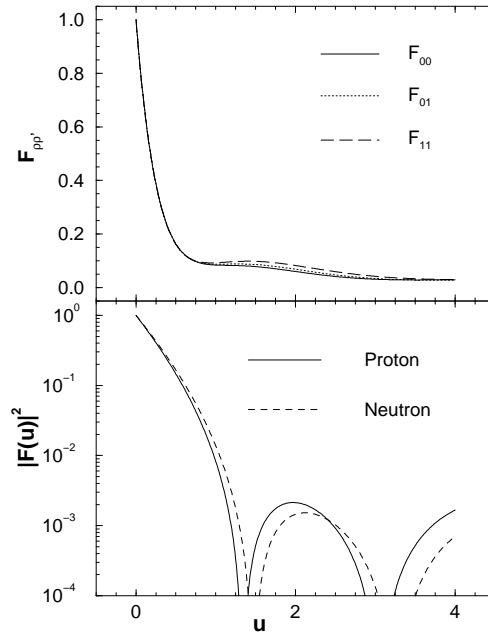


FIG. 4: Spin structure functions and squared proton and neutron form factor for ^{73}Ge .

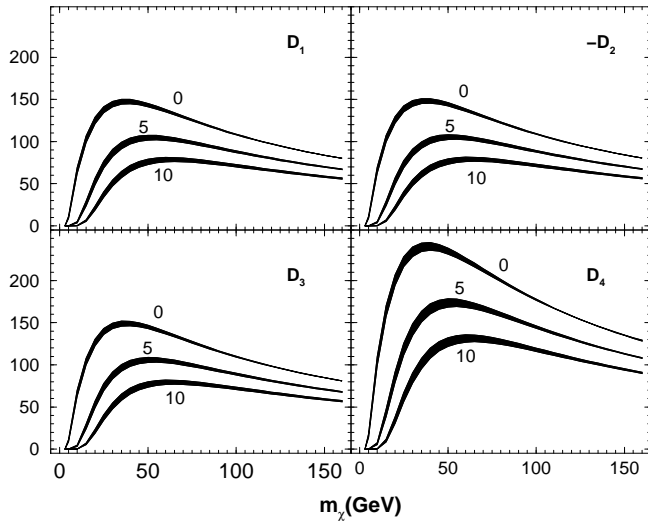


FIG. 5: Nuclear structure coefficients D_n of Eq. 14 plotted as a function of the WIMP mass. The graphs are plotted for three values of the detector threshold Q_{thr} namely $Q_{thr} = 0, 5, 10$ keV. The close lying graphs for each value of Q_{thr} represent the annual modulation.

i

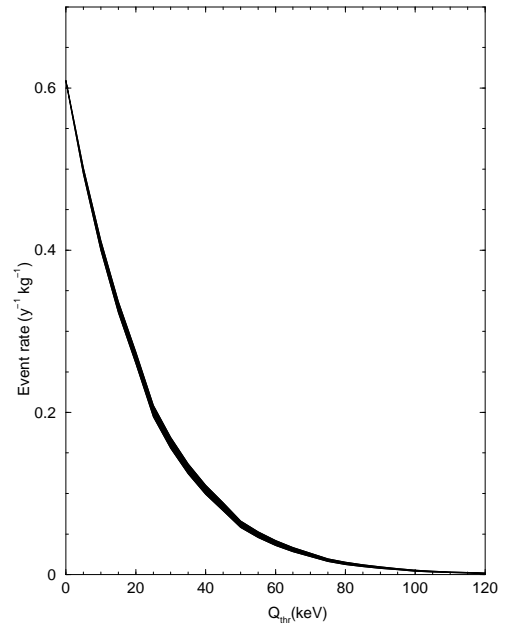


FIG. 6: The even rate in units of $\text{yr}^{-1}\text{kg}^{-1}$ as a function of detector threshold Q_{thr} . The thickness of the curve represents the annual modulation.

ouras, Phys. Rev. C **61**, 054612 (2000).
 [7] P. Pirinen, P.C. Srivastava, J. Suhonen and M. Kortelainen, Phys. Rev D **93**, 095012 (2016).
 [8] P. Toivanen, M. Kortelainen, J. Suhonen and J. Toivanen, Phys. Rev. C **79**, 044302 (2009).
 [9] D.S. Akerib et al., Phys. Rev. D **72**, 052009 (2005).
 [10] A. Broniatowski et al., Phys. Lett. B **681**, 305 (2009).
 [11] K. Freese, M. Lisanti and C. Savage, Rev. Mod. Phys. **85**, 1561 (2013).
 [12] R. Bernabei et al. Eur. Phys. J. C **73**, 2648 (2013).

[13] V.K.B. Kota and R. Sahu, Structure of Medium Mass Nuclei: Deformed Shell Model and Spin-Isospin Interacting Boson Model (CRC Press, Taylor and Francis group, Florida, 2016).
 [14] P.C. Srivastava, R. Sahu and V.K.B. Kota, Eur. Phys. J. A **51**:3, 2015.
 [15] R. Sahu, P.C. Srivastava and V.K.B. Kota, J. Phys. G **40**, 095107 (2013).
 [16] R. Sahu and V.K.B. Kota, Int. J. Mod. Phys. E **24**,

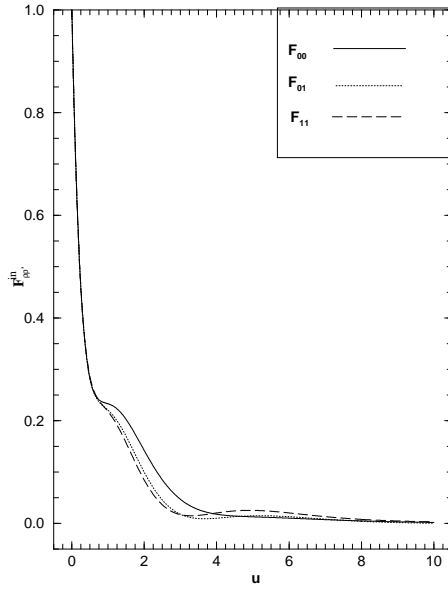


FIG. 7: Spin structure function in the inelastic channel

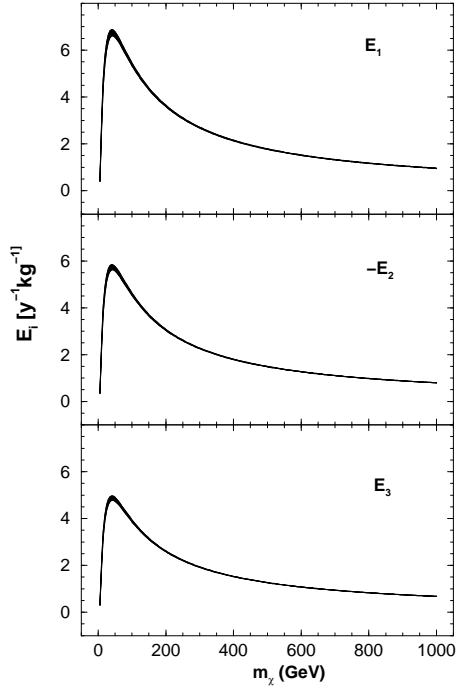


FIG. 8: Nuclear structure coefficients E_n in the inelastic channel. The thickness of the graphs represent annual modulation

- 1550022 (2015).
- [17] T.S. Kosmas, A. Faessler and R. Sahu, Phys. Rev C **68**, 054315 (2003)
- [18] R. Sahu and V.K.B. Kota, Phys. Rev. C **66**, 024301 (2002).
- [19] R. Sahu and V.K.B. Kota, Phys. Rev. C **67**, 054323 (2003).
- [20] S. Mishra, R. Sahu, and V.K.B. Kota, Prog. Theo. Phys. **118**, 59 (2007).
- [21] M. Kortelainen, T.S. Kosmas, J. Suhonen and J. Toivanen, Phys. Lett. B **632**, 226 (2006).
- [22] E. Holmlund et al., Phys. Lett. B **584**, 31 (2004).
- [23] J. Menendez, D. Gazit and A. Schwenk, Phys. Rev. D **86**, 103511 (2012).
- [24] P. Klos, J. Menendez, D. Gazit and A. Schwenk, Phys. Rev. D **88**, 083516 (2013).
- [25] L. Baudis et al. Phys. Rev. D **88**, 115014 (2013).
- [26] L. Vietze et al. Phys. Rev. D **91**, 043520 (2015).
- [27] <http://www.nndc.bnl.gov/ensdf>
- [28] J.J. Sun et al. Phys. Rev. C **92**, 054302 (2015).
- [29] M. Ted Ressel et al. Phys. Rev. D **48**, 5519 (1993).
- [30] C. Aalseth et al. (CoGent Collaboration), Phys. Rev. D **88**, 012002 (1913).
- [31] E. Aprile et al. (XENON100 Collaboration) Astopart. Phys. **35**, 573 (2012).
- [32] G. Angloher et al. Eur. Phys. J. C **72**, 1971 (2012).